

ASCA observations of deep ROSAT fields I. the nature of the X-ray source populations

I. Georgantopoulos¹, G.C. Stewart¹, A.J. Blair¹, T. Shanks², R.E. Griffiths³,
B.J. Boyle⁴, O. Almaini⁵, N. Roche⁶

¹ Department of Physics & Astronomy, The University of Leicester, Leicester LE1 7RH

² Physics Department, University of Durham, South Road, Durham DH1 3LE

³ Department of Physics, Carnegie Mellon University, Wean Hall, 5000 Forbes Ave., Pittsburgh, PA 15213 U.S.A.

⁴ Anglo-Australian Observatory, PO Box 296, Epping NSW 2121, Australia

⁵ Institute of Astronomy, Madingley Road, Cambridge CB3 0HA

⁶ Johns Hopkins University, Department of Physics & Astronomy, Baltimore, MD 21218, U.S.A.

25 September 2018

ABSTRACT

We present *ASCA* GIS observations (total exposure ~ 100 -200 ksec) of three fields which form part of our deep *ROSAT* survey. We detect 26 sources down to a limiting flux (2-10 keV) of $\sim 5 \times 10^{-14}$ erg cm $^{-2}$ s $^{-1}$. Sources down to this flux level contribute ~ 30 per cent of the 2-10 keV X-ray background. The number-count distribution, $\log N - \log S$, is a factor of three above the *ROSAT* counts, assuming a spectral index of $\Gamma = 2$ for the *ROSAT* sources. This suggests the presence at hard energies of a population other than the broad-line AGN which contribute to the *ROSAT* counts. This is supported by spectroscopic observations that show a large fraction of sources that are not obvious broad-line AGN. The average 1-10 keV spectral index of these sources is flat $\Gamma = 0.92 \pm 0.16$, significantly different than that of the broad-line AGN ($\Gamma = 1.78 \pm 0.16$). Although some of the Narrow Emission Line Galaxies which are detected with *ROSAT* are also detected here, the nature of the flat spectrum sources remains as yet unclear.

1 INTRODUCTION

The origin of the diffuse X-ray emission, the X-ray background (XRB), that dominates the sky from energies of 0.1 keV up to 1 MeV remains uncertain. The bulk of the XRB cannot originate from hot intergalactic gas (Mather et al. 1990) but instead must arise in discrete sources (for a review see Fabian & Barcons 1992). At soft energies (< 2 keV) great strides have been made after the launch of the X-ray satellite *ROSAT* (Trümper 1990). Deep observations with the *ROSAT* PSPC (Shanks et al. 1991, Hasinger et al. 1993, Branduardi-Raymont et al. 1994, Georgantopoulos et al. 1996) reveal a high density of X-ray sources (> 400 deg $^{-2}$, at 2×10^{-15} erg cm $^{-2}$ s $^{-1}$), which contribute over than half of the soft (0.5-2 keV) XRB. The integral number-count distribution, $\log N - \log S$, turns over to a flatter than Euclidean power law slope at $S_{0.5-2\text{keV}} \approx 2 \times 10^{-14}$ erg cm $^{-2}$ s $^{-1}$, tending to a slope of $\gamma \sim 1$ (Hasinger et al. 1993, Vikhlinin et al. 1995). Spectroscopic follow-up observations have shown that the majority of the sources are broad-line, type I AGN, ie QSOs and Seyfert 1 galaxies, at a mean redshift of $z=1.5$ (e.g. Shanks et al. 1991, Boyle et al. 1995, Carballo et al. 1995, Georgantopoulos et al. 1996, Bower et al. 1996). However, the QSO luminosity function, the anisotropy of the XRB and the average QSO spectra argue strongly against a

QSO origin for the soft XRB. The QSO luminosity function and its evolution has been derived using combined *Einstein* and *ROSAT* data (Boyle et al. 1993, 1994). An integrated QSO contribution of only ~ 50 per cent in the 0.5-2 keV band is determined. A similar conclusion is reached from studies of the XRB anisotropy. The auto-correlation function (ACF) of the 1-2 keV XRB presents a weak signal (Georgantopoulos et al. 1993, Soltan & Hasinger 1994, Chen et al. 1994) which lies below the strong ACF signal predicted from the optical QSO correlation function (Shanks & Boyle 1994, Georgantopoulos & Shanks 1994). Finally, the average QSO spectra in deep *ROSAT* fields have a photon spectral index of $\Gamma \sim 2$ (Stewart et al. 1994, Almaini et al. 1996), steeper than the spectrum of the XRB ($\Gamma \sim 1.5$) at soft energies (Georgantopoulos et al. 1996). This extends the spectral paradox already noted in harder X-rays (Boltdt 1987) and suggests either a population with a flat spectral index or one which is heavily absorbed and remains unidentified at faint fluxes. Indeed, *ROSAT* PSPC exposures reveal a new population of X-ray luminous ($L_x \gtrsim 10^{42}$ erg s $^{-1}$) optically faint galaxies, (Roche et al. 1995, Griffiths et al. 1995, Boyle et al. 1995, Carballo et al. 1995, Georgantopoulos et al. 1996, Griffiths et al. 1996) which do not have the broad emission lines typical of QSOs. Although these narrow emission line galaxies (NELGs) are too faint for individual X-ray spectral

analysis, their co-added spectra appear to be flat ($\Gamma \sim 1.5$), similar to the XRB spectrum in the same energy band (Almaini et al. 1996, Romero-Colmenero et al. 1996). Strong positive cross-correlation signals between the PSPC background fluctuations and faint galaxies ($B < 23$) have shown that these contribute a significant fraction (at least 17 per cent) of the soft XRB (Roche et al. 1995).

On the other hand, the hard XRB (> 2 keV), where the bulk energy density resides, remains less well explored, as measurements at hard X-rays have been performed mainly using collimated X-ray detectors with coarse (degrees) angular resolution. The *HEAO-1* experiment (Wood et al. 1984) has detected several hundred sources over the whole sky, in the 2-10 keV band, with fluxes $\gtrsim 5 \times 10^{-12}$ erg cm $^{-2}$ s $^{-1}$, contributing less than 5 per cent of the hard XRB intensity. The logN-logS from *HEAO-1* (Piccinotti et al. 1982) and *Ginga* (Kondo 1990) is represented by a Euclidean power law with a normalization a factor of 2-3 above that of the *ROSAT* logN-logS. The fluctuations analysis of the hard XRB in *Ginga* fields (Butcher et al. 1997) extends these conclusions down to flux levels of 5×10^{-13} erg cm $^{-2}$ s $^{-1}$. These imply that a flat spectrum ($\Gamma \lesssim 1.5$) or absorbed population ($N_H > 3 \times 10^{21}$ cm $^{-2}$) dominates the hard energies (e.g. Ceballos & Barcons 1996). The majority of the bright hard X-ray sources are nearby type I AGN (Piccinotti et al. 1982). They have a power law spectrum of $\Gamma \sim 1.7$ (e.g. Nandra & Pounds 1994) inconsistent with the XRB spectrum in this band which has a spectral index of $\Gamma \sim 1.4$ (Marshall et al. 1980, Gendreau et al. 1995).

The launch of the X-ray satellite *ASCA* provides the first opportunity to observe the hard (2-10 keV) X-ray sources down to a flux level of few times 10^{-14} erg cm $^{-2}$ s $^{-1}$, about two orders of magnitude fainter than the *HEAO-1* survey, but still an order of magnitude above the flux limit of the deepest *ROSAT* surveys. Here, we present the results from *ASCA* observations of three fields included in our deep *ROSAT* survey (Shanks et al. in preparation). The benefits of observing *ROSAT* fields with previous spectroscopic follow-up observations are obvious, as we can immediately obtain the optical identifications for many of the *ASCA* sources. The major aim of this paper is to examine the nature of the the faint hard X-ray sources and to estimate their contribution to the XRB. First, we discuss the X-ray and optical properties of the detected sources and then we derive their number-count distribution, logN-logS, as well as their contribution to the hard XRB.

2 THE X-RAY OBSERVATIONS

2.1 Data reduction

Our deep *ROSAT* survey (Shanks et al.; in preparation) consists of 7 PSPC fields with exposure times up to 80 ksec and covers ~ 2 deg 2 . About 300 sources have been detected down to a flux limit of 3×10^{-15} erg cm $^{-2}$ s $^{-1}$ (0.5-2 keV) in the central 20 arcmin radius of the PSPC field-of-view where the detector/telescope sensitivity is the highest. Both the optical and the X-ray observations from the first 5 fields are described in detail in Georgantopoulos et al. (1996).

Three fields from our *ROSAT* survey (QSF3, GSGP4, BJS855) have been observed with the *ASCA* satellite

Table 1. List of *ASCA* fields

Field	α	δ	N_H (10^{20} cm $^{-2}$)	Exposure (ksec)
QSF3	03 41 44.4	-44 07 04.8	1.7	109
GSGP4	00 57 25.2	-27 37 48.0	1.8	50
BJS855	10 46 24.0	-00 20 38.4	1.8	54

(Tanaka et al. 1994). *ASCA* was launched in February 1993 and carries two SIS (Solid State Imaging Spectrometer) and two GIS (Gas Imaging Spectrometer) each with its own X-ray telescope (XRT) (Serlemitsos et al. 1995). The SIS instruments cover a field-of-view of approximately 20x20 arcmin whilst the GIS instruments cover an area of 20 arcmin radius. Here we present the analysis of the GIS data alone because a) the GIS field-of-view matches that used in our *ROSAT* survey and b) with the GIS we maximize the effective exposure times, ie the net exposure times after rejecting time periods with high rates of particle events. In table 1 (please note that this table will not be distributed before the actual publication of the paper) we give the field names in column (1); equatorial coordinates (J2000), in columns (2) and (3); the hydrogen column density in units of 10^{20} cm $^{-2}$ (Stark et al. 1992) in column (4); finally the effective exposure times per telescope in ksec are given in column (5). The QSF3 field was observed four times during the period of Performance Verification (PV phase). The first observation was in June 1993 and the remaining three in September 1993. The GSGP4 and the BJS855 fields were observed in June 1994 and November 1995 respectively.

Images are created in sky coordinates using the FTOOLS/XSELECT software (Day et al. 1995). We reject a small fraction of the data that corresponds to times of high particle background, keeping only data which satisfied the following selection criteria: a) elevation angle from the Earth limb greater than 5 degrees b) the satellite remains outside the South Atlantic Anomaly c) the Radiation Belt Monitor gives values below 200 ct s $^{-1}$. Finally, a bright ring around the edge of the field-of-view that contains mostly particle background events is removed from the image (see Day et al. 1995).

The nominal energy response of the GIS+XRT combination is 0.8-12 keV. However, below 1 keV and above 10 keV the response drops rapidly. Here, we use the 2-10 keV band for our source detection. The 1-2 keV overlaps with the *ROSAT* PSPC energy response and it is used to check the *ASCA* results against the well calibrated *ROSAT* data. The Point Spread Function (PSF) of the GIS+XRT combination has a half-power-radius of 1.5 arcmin on-axis. The radius of the encircled energy fraction depends on the off-axis angle. The 2 arcmin radius includes ~ 60 per cent of the source light on-axis while at 17 arcmin this fraction reduces to ~ 40 per cent (e.g. Takahashi et al. 1995).

We mosaic the images from the two detectors GIS2 and GIS3 in order to increase the exposure time and hence to maximize the signal-to-noise ratio for source detection. As the optical axes of the two telescopes do not coincide, the maximum exposure times are not simply double the expo-

sure times given in table 1. The maximum exposure times in the mosaic fields are approximately 185, 95 and 100 ksec for QSF3, GSGP4 and BJS855 respectively. The background appears to be uniform, within 17-18 arcmin radius, despite the strong vignetting of the XRT telescope (only ~ 30 per cent of the light is captured at an off-axis angle of 18 arcmin, Serlemitsos et al. 1995). The lack of vignetting in the images is attributed to stray light contamination from outside the field-of-view (e.g. Gendreau 1995) and to a particle background component which increases with off-axis angle (Kubo et al. 1994).

We use the Point Source Search (PSS) algorithm (Allan 1992) to select candidate sources in the full 20 arcmin radius field-of-view, down to a low level of significance (3σ). PSS detects peaks above a given threshold and fits the PSF to the observed surface brightness distribution to decide whether these peaks are real sources or simply Poissonian fluctuations. In addition, we run the PISA source detection algorithm (Draper & Eaton 1995) to check whether any sources (especially confused or double sources) have been missed by the PSS. Finally, we include in our source list only the sources, detected by either the above two algorithms, whose counts in a detection cell of 1 arcmin exceed the 4σ background fluctuations. At this level, only ~ 0.1 spurious sources are expected in our survey. At faint fluxes confusion may start posing problems. A lower limit on the number of confused sources is found as follows. The *Ginga* fluctuations $\log N - \log S$ (Butcher et al. 1997) predicts a surface density of $\sim 50 \text{ deg}^{-2}$ at the flux limit of our survey ($\sim 5 \times 10^{-14} \text{ erg cm}^{-2} \text{ s}^{-1}$), translating to 0.014 sources per 1 arcmin radius beam or ~ 0.4 double sources per field. Sources fainter than the flux limit of our survey exacerbate the confusion. Of course, if the $\log N - \log S$ flattens from Euclidean, as is the case in soft X-rays, confusion problems will be relaxed.

A total of 26 point sources (there is no significant evidence for extension) were detected in our 3 *ASCA* fields: 10 in the QSF3 field, 9 in the GSGP4 and 7 in the BJS855 field. The flux limit in the QSF3 field is deeper, by about 30 per cent, compared to the other two fields. Hence, we expect to detect ~ 50 per cent more sources in QSF3, assuming an integral $\log N - \log S$ slope of $\gamma = 1.5$; this translates to 10-14 sources in agreement with our observed number. Therefore, there is no evidence for large field-to-field fluctuations in the number of sources detected. Note that the upper limit on the fluctuations in the 2-10 keV band from the *HEAO-1* all-sky survey is 5 per cent on few degree scales (see Fabian & Barcons 1992).

Count rates were estimated as follows. In most cases, we measure the source counts in a 1 arcmin radius. This radius contains about 30 per cent of the source counts on-axis. As most of our sources are faint, with less than 50 counts in the 1 arcmin radius detection cell, use of a larger radius would increase the source flux errors. For the few relatively bright sources, we use a radius of 2 arcmin. We then subtract the background counts as measured in a nearby 'source free' region. Count rates are calculated using the exposure maps of the mosaic images; The faintest source has a count rate of $\sim 8 \times 10^{-4} \text{ ct s}^{-1}$.

Table 2. Cumulative number of *ASCA-ROSAT* cross-correlations vs. separation R

$< R$ (arcsec)	ROSAT 5σ		ROSAT 4σ	
	Obs.	Exp.	Obs.	Exp.
30	5	0.7	6	1.0
45	15	1.7	17	2.2
60	17	3.0	20	3.9
75	18	4.5	23	6.1
90	21	6.5	29	8.5

2.2 The source list

We cross-correlate the *ASCA* hard (2-10 keV) source positions with those from the *ROSAT* PSPC (0.5-2 keV). These cross-correlations provide us immediately with the optical identifications for most *ASCA* sources, since a large fraction (~ 75 per cent) of our *ROSAT* survey sources have been spectroscopically identified. 18 *ASCA* sources have counterparts in the 5σ *ROSAT* list (see Georgantopoulos et al. 1996), within 90 arcsec radius. As the rms error on the *ASCA* positions is ~ 50 arcsec (see below), we expect ~ 95 per cent of our *ASCA* X-ray centroids to lie within 90 arcsec radius. Only three of the sources have two, 5σ , *ROSAT* counterparts within the above radius. In these cases, we assumed that the real counterpart is the nearest source; the details are given in table 3 below. Five more *ASCA* sources have counterparts in the deeper 4σ *ROSAT* list. Finally, three hard X-ray sources have no *ROSAT* PSPC counterparts. We note that due to the high density of *ROSAT* sources (typically $\sim 150 \text{ deg}^{-2}$ at our faint flux limits) a few of the above cross-correlations may be chance coincidences, especially those at large separation. The cumulative number of *ASCA-ROSAT* (2-10 keV vs. 0.5-2 keV) cross-correlations as a function of separation in arcsec is given in table 2 for both the 5σ and the 4σ *ROSAT* lists. The expected number of objects, assuming that the *ROSAT* sources are distributed randomly with respect to the *ASCA* sources, is given as well. Note however, that the above estimate of the number of random coincidences is conservative since we do not exclude the *ROSAT* sources that may have a true *ASCA* counterpart in the calculation of the number density of random *ROSAT* sources. The above cross-correlation gives an rms error for the *ASCA* GIS positions of ~ 50 arcsec.

We give the list of sources detected in the hard 2-10 keV band in table 3. The source name is given in column (1); columns (2) and (3) give the *ASCA* and *ROSAT* equatorial (J2000) coordinates for each object; the offset between the *ASCA* and *ROSAT* positions is listed in column (4), in arcsec; column (5) contains the *ASCA* GIS count rate in the 2-10 keV band together with the photon errors in units of ($10^{-3} \text{ ct s}^{-1}$); columns (6) and (7) contain the soft *ROSAT* PSPC and *ASCA* GIS flux (1-2 keV) in units of $10^{-14} \text{ erg cm}^{-2} \text{ s}^{-1}$. We converted the 1-2 keV count rates to fluxes using a spectral index of $\Gamma = 1.7$ for all objects. Of course, this is not strictly true for all objects. However, the choice of spectral index affects very little the resulting flux due to the very narrow spectral band. The conversion factors are then 2×10^{-11} and $1.2 \times 10^{-11} \text{ erg cm}^{-2} \text{ ct}^{-1}$ for

GIS and PSPC respectively. If the object is not detected in the GIS 1-2 keV band down to the 3σ detection threshold, the 3σ upper limit is quoted (see Kraft, Burrows & Nousek 1991). Finally column (8) contains the optical identification and redshift where available. An outline of the optical observations and identification procedure of our *ROSAT* survey are given in Georgantopoulos et al. (1996) while the full details will be published elsewhere (Shanks et al, in preparation). We denote with asterisk (*) the sources detected in the low significance (4σ) *ROSAT* list. The sources denoted with question-mark (?) were too faint optically (typically $B > 22$) to give good signal-to-noise optical spectra. Three sources were not spectroscopically observed due to fibre positioning restrictions. Note that there are appreciable differences between the *ROSAT* and *ASCA* soft 1-2 keV flux. Although some variability in QSOs might be expected, in other cases it could point towards a possible misidentification, as for example in the case of AXJ0057.6-2731. At low fluxes the errors are expected to be significant: typical errors from photon statistics alone are of the order of 40 per cent for the faintest sources in the QSF3 field.

From table 3 we see that several QSOs are detected; their mean redshift is $z \approx 1.1$. Two clusters are also detected. One of those, AXJ0057.0-2741 is a high redshift cluster ($z=0.561$); its soft X-ray properties are discussed in Roche et al (1995). We have also identified a number of galaxies as potential counterparts to the *ASCA* sources. One (AXJ1047.2-0028) is classified as an early type galaxy, on the basis of absorption features in its optical spectrum; its redshift is $z=0.08$ while its luminosity, $L_x \approx 2 \times 10^{42}$ erg s^{-1} , albeit high is not atypical of early-type galaxies detected by Einstein and *ROSAT* (e.g. Fabbiano 1989). We have also identified four NELGs with luminosities ranging from $L_x \sim 10^{42}$ to 10^{44} erg s^{-1} . Despite the presence of several galaxies in our *ASCA* survey, we note that a significant galaxy contribution to the hard X-ray background cannot yet be firmly established, due to the poor statistics. Most NELGs are faint *ROSAT* sources ($< 5\sigma$) and thus the possibility that some are due to chance coincidences cannot be ruled out.

2.3 The hardness ratios

Additional clues on the origin of the faint X-ray sources come from their hardness ratios. Here, we define the *average* hardness ratio as, $h - s / h + s$, where h and s are the total number of counts in the detection cells, in the 2-10 and 1-2 keV bands respectively, for a given group of sources. A detailed analysis of the combined *ASCA* and *ROSAT* spectra is given in Georgantopoulos et al. (in preparation). The hardness ratio of all sources (excluding the star) is 0.23 ± 0.04 . We convert the hardness ratios to photon indices using XSPEC at a mean off-axis angle of 8 arcmin. The resulting spectral index is $\Gamma = 1.30 \pm 0.10$ (1σ error). The hardness ratio of the galaxies and unidentified sources, i.e. excluding the identified QSOs, the two clusters and the star, has a value of 0.38 ± 0.06 corresponding to an index of $\Gamma = 0.92 \pm 0.16$. This is flatter than the spectral index of the 2-10 keV XRB, which has $\Gamma \sim 1.4 - 1.5$ (Gendreau et al. 1995, Chen, Fabian & Gendreau 1997). Hence, these objects may be the first faint examples of the hard spectrum population that makes a substantial contribution to the hard XRB. In contrast, the

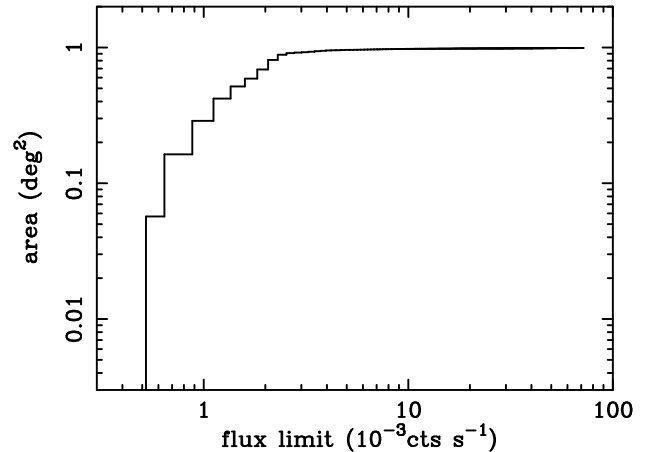


Figure 1. The sky coverage of our survey as a function of limiting count rate.

average QSO hardness ratio is 0.04 ± 0.06 yielding a spectral index of $\Gamma = 1.78 \pm 0.16$, marginally flatter than the average *ROSAT* QSO spectral index in our fields (Stewart et al. 1994) but similar to the average nearby AGN spectrum in this band (Nandra & Pounds 1994). Chen et al. (1997) present *ASCA* SIS observations of the two bright QSOs in the QSF3 field. The combined SIS+PSPC fits give spectral indices of $\Gamma \approx 3.1 \pm 0.1$. This spectral index is considerably steeper than ours, possibly due to the lower energy range of the *ASCA* SIS and *ROSAT* PSPC which can be affected by soft excesses in the QSO spectra. However, both their work and ours suggest that the average QSO spectra are steeper than that of the XRB. This result, the spectral paradox, was noted earlier with *HEAO-1* (e.g. Boldt 1987) and *Ginga* albeit at much brighter fluxes ($> 7 \times 10^{-12}$ erg cm^{-2} s^{-1}).

3 THE NUMBER-COUNT DISTRIBUTION

3.1 The 2-10 keV logN-logS

We calculate the extragalactic number-count distribution, $\log N - \log S$, in the 2-10 keV band. We use the 25 sources detected in our three fields, excluding only the star in the QSF3 field. Due to the strong vignetting of the XRT, the faintest sources can only be detected in the center of the GIS field-of-view, where the sensitivity is the highest, while the bright sources can be detected at all off-axis angles. Therefore, we need first to estimate the sky coverage of our survey. The cumulative area covered as a function of the limiting flux is given in Fig. 1.

The integral number-counts, $N(> S)$, are given by the sum $\Sigma(1/\Omega_i)$, where Ω_i is the area coverage at the flux, S_i , of the source i . To facilitate comparison with previous results we use a spectral index of $\Gamma = 1.7$; this corresponds to a count-rate-to-flux conversion factor of 5.8×10^{-11} erg cm^{-2} ct^{-1} ; we note that the count-rate-to-flux conversion factor for our mean spectral index of $\Gamma \sim 1.3$ would be

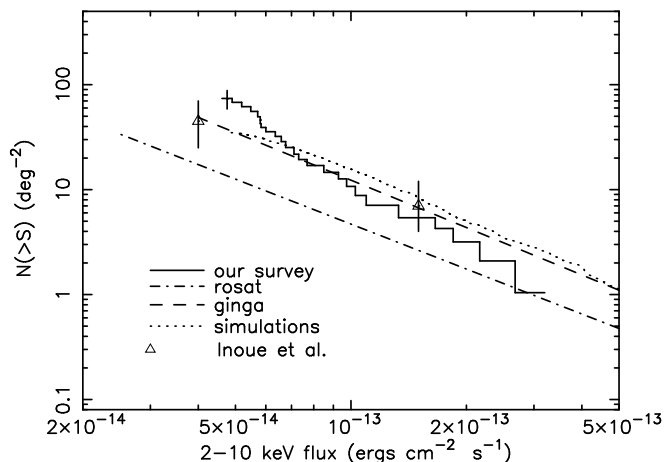


Figure 2. The derived integral $\log N - \log S$ in the 2-10 keV band from our survey (histogram). Also shown the *ROSAT* counts (dot-dashed line), converted in the 2-10 keV band using $\Gamma = 2$, the *Ginga* counts (dashed line), the $\log N - \log S$ derived from the 100 simulated ASCA fields (dotted line). The triangles are adapted from the Inoue et al. deep ASCA survey. All errors correspond to the 1σ confidence level.

$\approx 6.5 \text{ erg cm}^{-2} \text{ ct}^{-1}$. The resulting $\log N - \log S$ is plotted in Fig. 2 (histogram).

The preliminary number-counts from two deep, Japanese, *ASCA* surveys are adapted from Inoue et al. (1996) (triangles). We also plot the soft (0.5-2 keV) number-counts (dot-dash line), as derived from our *ROSAT* survey (Georgantopoulos et al. 1996), converted to the 2-10 keV band using a power-law index of $\Gamma = 2$ for the *ROSAT* source spectra (Hasinger et al. 1993, Vikhlinin et al. 1995b). The $\log N - \log S$ measured from the *Ginga* fluctuations (Butcher et al. 1997), is plotted as a dashed line. Finally, the dotted line gives the $\log N - \log S$ derived from 100 Monte Carlo simulations of *ASCA* fields (see below). All errors plotted correspond to the 1σ significance level. Inspection of Fig. 2 suggests the following. The $\log N - \log S$ of our *ASCA* survey appears to be in rough agreement with the Japanese *ASCA* surveys, especially at bright fluxes. Furthermore, the *ASCA* $\log N - \log S$ is in agreement with the number-counts measured from the *Ginga* fluctuations. Instead, the *ASCA* number-counts lie significantly above the *ROSAT* $\log N - \log S$. This excess number density of hard X-ray sources suggests that a new source population, other than the QSOs which dominate the soft $\log N - \log S$, is present in our *ASCA* survey. This population could remain undetected in the *ROSAT* surveys of comparable flux depth ($S_{0.5-2\text{keV}} > 10^{-14} \text{ erg cm}^{-2} \text{ s}^{-1}$) due to its flat or absorbed X-ray spectrum. However, we have first to rule out any possibility that systematic effects could alter the $\log N - \log S$ form and produce the observed excess density. Such effects in the source detection and flux estimation are examined in the next section.

3.2 Checking for systematic effects

The $\log N - \log S$ derived above may be affected by several systematic effects in the source detection and flux calculation procedure. The most important are the Eddington bias and source confusion. The Eddington bias is the net gain of sources near the flux limit of the survey due to flux errors. Murdoch, Crawford & Jauncey (1973) and Schmitt & Maccauro (1986) discuss this effect and give analytic corrections for pure power law counts. However, the above corrections assume that the flux error distribution is well determined. The Eddington bias is going to have a small effect in our $\log N - \log S$ estimation, either if the flux errors are negligible or alternatively, if the $\log N - \log S$ breaks to a flatter than Euclidean power law, as in the case of the *ROSAT* number-counts. Source confusion plays an important role at faint fluxes and may result in either the increase or the decrease of the total number of sources detected. If the confused sources are below the detection threshold, then the merged source may appear above the survey's flux limit and thus we end up with a net gain in the number of sources. Alternatively, two sources above the detection threshold could merge to form a brighter source, thus resulting in a loss of fainter sources.

We check the validity of our $\log N - \log S$ using two tests. We first derive the soft (1-2 keV), $\log N - \log S$, from our three *ASCA* GIS fields. Comparison with the well-determined *ROSAT* $\log N - \log S$ then provides powerful constraints on possible GIS systematic flux errors. Using the detection methods described earlier in this paper, we detect 15 sources in our three fields (of which two are identified as stars), in the 1-2 keV band down to a flux limit of $\sim 10^{-14} \text{ erg cm}^{-2} \text{ s}^{-1}$. The integral $\log N - \log S$ for the 13 sources, excluding the two stars, is plotted in Fig. 3. It is compared with the extragalactic 0.5-2 keV *ROSAT* $\log N - \log S$ (Georgantopoulos et al. 1996) converted to the 1-2 keV band using a spectral index of $\Gamma = 2$. Despite the poor statistics of the *ASCA* counts, we see that the two $\log N - \log S$ are in good agreement, demonstrating that the combined effects of flux errors and source confusion do not significantly change the $\log N - \log S$ at soft fluxes.

As an additional test, we performed Monte Carlo simulations of the 2-10 keV images. We create 100 fields in total, having the same exposures times, and background count rates as the three observed fields. In each field X-ray sources were assigned random positions, while their input fluxes were drawn from an integral $\log N - \log S$ with Euclidean slope ($\gamma = 1.5$) and a normalization of 390 deg^{-2} at $10^{-14} \text{ erg cm}^{-2} \text{ s}^{-1}$ in agreement with the *Ginga* counts. The faint limit of our simulation is $5 \times 10^{-15} \text{ erg cm}^{-2} \text{ s}^{-1}$, about an order of magnitude below the flux limit of our *ASCA* survey; at this flux level the $\log N - \log S$ saturates the 2-10 keV XRB. A uniform particle component is added with a count rate of $5 \times 10^{-5} \text{ ct s}^{-1}$ (e.g. Kubo et al. 1995). For each source the photons are spread using the actually measured PSF. Finally, the vignetting of the XRT (Serlemitsos et al. 1995) has been applied analytically. We apply exactly the same detection procedure, used in the case of the actual fields. We detect ~ 815 sources in total. The integral $\log N - \log S$ of the simulated fields was given in Fig. 2 (dotted line). We see that there is rough agreement between the simulations and the input $\log N - \log S$. This does not imply that flux

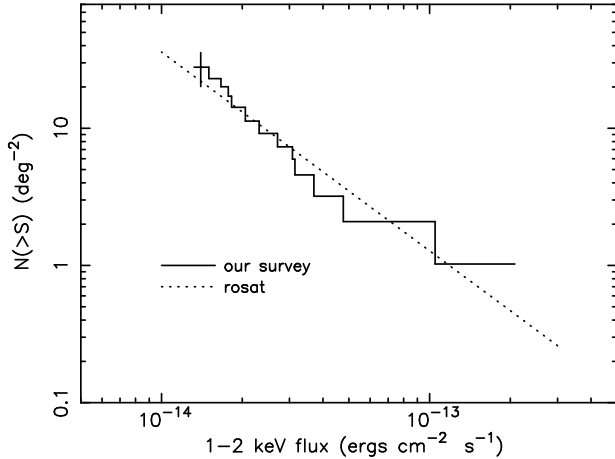


Figure 3. The integral $\log N - \log S$ of the *ASCA* soft sources detected in the 1-2 keV band (histogram) compared to the *ROSAT* 1-2 keV $\log N - \log S$.

errors are negligible. Our simulations show that flux errors as large as 100 per cent can be expected near the survey’s flux limit. It is therefore probable that the observed agreement between the simulated and input $\log N - \log S$ near the survey’s flux limit is because confusion approximately cancels out the Eddington bias effect.

3.3 Contribution to the XRB

The summed flux of the 10 sources in the deepest field, QSF3, is $\sim 8 \times 10^{-13}$ erg cm $^{-2}$ s $^{-1}$ in the 2-10 keV band. The total XRB flux in the same band is $\sim 6.5 \times 10^{-12}$ erg cm $^{-2}$ s $^{-1}$ deg $^{-2}$ (Chen et al. 1997). This translates to a resolved source contribution of 12 per cent. However, this is only a lower limit since it does not take into account the strong telescope vignetting which prevents the detection of faint sources at large off-axis angles. Instead, we need to estimate the source contribution by using the observed $\log N - \log S$ distribution. We fit a power law model ($dN \propto N^{-\beta}$) to the differential source counts (e.g. Murdoch et al. 1973). We find a slope of $\beta = 3.27 \pm 0.57$ (integral slope of 2.27), where the errors quoted correspond to the 90 per cent confidence level. We note that a Euclidean slope cannot be ruled out at the $\sim 2\sigma$ confidence level. Given the limited statistics and the small flux range covered by our survey, we conclude that there is no strong evidence yet for a non-Euclidean count distribution. Fixing the integral $\log N - \log S$ slope to the Euclidean value of 1.5 gives a normalization of 4.4×10^{-19} deg $^{-2}$ (erg cm $^{-2}$ s $^{-1}$) $^{1.5}$ comparable to the *Ginga* normalization. Using the above $\log N - \log S$ ($\gamma = 1.5$), we estimate a source contribution of ~ 13 keV cm $^{-2}$ s $^{-1}$ sr $^{-1}$ (2-10 keV) down to the limiting flux of our survey or about 30 per cent of the observed XRB in this band. Extrapolation of our counts down to 5×10^{-15} erg cm $^{-2}$ s $^{-1}$, i.e. an order of magnitude fainter than the limiting flux of the present survey and at comparable flux depth to the deep *ROSAT* surveys, produces all the XRB.

Our best fit slope of $\gamma = 2.27$ gives a contribution of over 40 per cent down to the flux limit of our survey while it saturates the XRB at a flux of $\sim 2 \times 10^{-14}$ erg cm $^{-2}$ s $^{-1}$. The above calculations show that future X-ray missions like *JET-X*, *XMM* and *AXAF* will be able to resolve the hard XRB, unless the counts turn over to a flatter slope, at fluxes fainter than the flux limit of our survey.

We finally note that although *HEAO-1* and *ASCA* observations have shown that the slope of the hard XRB is in the range $\Gamma = 1.4 - 1.5$ in the 1-10 keV band, its exact normalization is not yet well determined. In our calculations above, we use the measurements of the XRB from the *ASCA* SIS observations of the QSF3 field (Chen et al. 1997). These give a normalization of 10.5 ± 0.4 keV cm $^{-2}$ s $^{-1}$ sr $^{-1}$ keV $^{-1}$, at 1 keV, consistent with our *ROSAT* XRB measurements of the same field (Georgantopoulos et al. 1996) and other *ROSAT* fields. *ASCA* GIS observations of various fields (Ishisaki 1996) give similar values for the normalization. However, *ASCA* SIS observations (Gendreau et al. 1995) yield a somewhat lower value for the XRB (9 keV cm $^{-2}$ s $^{-1}$ sr $^{-1}$ keV $^{-1}$ at 1 keV) closer to the *HEAO-1* measurements (Marshall et al. 1980). If we use instead the Gendreau et al. (1995) value, our number-count distribution ($\gamma = 1.5$) saturates the XRB at even higher fluxes (7×10^{-14} erg cm $^{-2}$ s $^{-1}$).

4 CONCLUSIONS

We have discussed deep *ASCA* GIS observations of three fields from the deep *ROSAT* survey of Shanks et al. (in preparation). We detected 26 sources down to a limiting flux of $\sim 5 \times 10^{-15}$ erg cm $^{-2}$ s $^{-1}$ (2-10 keV). In the deepest field these sources contribute about 30 per cent of the XRB, as measured by Chen et al. (1997). There appears to be an excess density of hard X-ray sources of about a factor of three above the *ROSAT* counts. The agreement of the *ASCA* and *ROSAT* soft (1-2 keV) $\log N - \log S$ as well as Monte Carlo simulations suggest that this excess is not an artefact of flux errors or confusion at faint fluxes. Our finding confirms and extends previous *HEAO-1* and *Ginga* results at much brighter fluxes. The observed hard X-ray source excess density suggests that a population, other than the QSOs that dominate the soft (0.5-2 keV) source counts, remains unidentified at hard X-rays. This population must have a flat or absorbed X-ray spectrum since it is not detected in the *ROSAT* band at comparable, bright, flux levels i.e. $> 10^{-14}$ erg cm $^{-2}$ s $^{-1}$. Indeed, previous spectroscopic observations of our *ROSAT* survey at the Anglo-Australian Telescope show a relatively low fraction of QSOs among the hard X-ray sources: we detect 8 QSOs, 2 clusters, 1 star while 6 sources coincide with NELGs or early-type galaxies. The remaining 9 sources are unidentified. Although we cannot yet conclusively rule out the possibility that some of the 9 unidentified sources are broad-line AGN, the average hardness ratio of the 15 galaxies and unidentified sources yields a spectral index of $\Gamma = 0.92 \pm 0.16$, significantly different from the QSO spectral index ($\Gamma \approx 1.78 \pm 0.16$) and flatter than the XRB spectral index ($\Gamma \sim 1.4$). This corroborates the presence of a new flat spectrum population that could produce a large fraction of the hard XRB. Nevertheless, the nature of this population remains unknown. *ROSAT* observations have de-

tected a large number of NELGs at faint fluxes (Roche et al. 1995, Griffiths et al. 1995, 1996, Boyle et al. 1995), which may be associated with obscured active nuclei or starforming galaxies. Narrow-line type 2 AGN are also detected in *ASCA* surveys (e.g. Ohta et al. 1996). In our *ASCA* survey we find a relatively large number of NELGs and early-type galaxies. However, we emphasize yet again that due to the large positional error box of the *ASCA* detectors, a few of these identifications may be due to chance coincidences. Therefore, the amount of the NELG contribution at hard X-rays remains yet unknown.

In conclusion, our *ASCA* survey has succeeded in resolving and identifying a large fraction (~ 30 per cent) of the hard 2-10 keV XRB. Although some QSOs are detected, *ASCA* has clearly detected another population with a flat hard X-ray spectrum. Although there are hints that this could be associated with NELGs, the limited statistics of the present survey, together with the large positional errors of the *ASCA* GIS hinder the identification of this new population. Further *ASCA* or *SAX* observations, of fields previously observed by *ROSAT*, together with spectroscopic follow-up observations of the unidentified sources are necessary to clarify the nature of the hard X-ray population.

ACKNOWLEDGEMENTS

We are grateful to Ian Hutchinson for his help on the *ASCA* simulation software. We would like to thank the referee Xavier Barcons for many useful comments and suggestions. This research has made use of data obtained through the LEDAS and HEASARC online services, provided by the Leicester University and the NASA Goddard Space flight Center respectively. The optical data were obtained at the Anglo-Australian telescope. IG, GCS and OA acknowledge the support of PPARC.

REFERENCES

- Allan, D.J., 1992, Starlink ASTERIX User Note 004
 Almaini O., Shanks T., Roche N., Griffiths R.E., Boyle B.J., Stewart G.C., Georgantopoulos I., 1996, MNRAS, 282, 295
 Boldt, E., 1987, Phys. Rep., 146, 215
 Boyle B.J., Griffiths R.E., Shanks T., Stewart G.C., Georgantopoulos I., 1993, MNRAS, 260, 925
 Boyle B.J., Griffiths R.E., Shanks T., Stewart G.C., Georgantopoulos I., 1994, MNRAS, 271, 639
 Boyle B.J., McMahon R.G., Wilkes B.J., Elvis, M., 1995, MNRAS, 272, 462
 Bower, R.G. et al., 1996, MNRAS, 281, 59
 Branduardi-Raymont, G. et al., 1994, MNRAS, 270, 947
 Butcher, J.A., et al., 1997, MNRAS, in press
 Carballo R., Warwick R.S., Barcons X., Gonzalez-Serrano J.I., Barber C.R., Martinez-Gonzalez E., Perez-Fournon I., Burgos J., 1995, MNRAS, 277, 1312
 Ceballos, M.T., Barcons, X., 1996, MNRAS, 282, 493
 Chen L.-W., Fabian A.C., Warwick, R.S., Branduardi-Raymont G., Barber C.R., 1994, MNRAS, 266, 846
 Chen L.-W., Fabian A.C., Gendreau K.C., 1997, MNRAS, 285, 449
 Day C., Arnaud K.A., Ebisawa K., Gotthelf E., Ingham, J., Mukai K., White N., 1995, The ABC Guide to ASCA data, v. 4, ASCA Guest Observer Facility, NASA
 Draper, P.W., Eaton, N., 1995, Starlink User Note 109.6
 Fabbiano, G., 1989, ARA&A, 27, 87
 Fabian A.C., Barcons X., 1992, ARA&A, 30, 429
 Gendreau K. et al. 1995, PASJ, 47, L5
 Georgantopoulos, I., Shanks, T., 1994, MNRAS, 271, 773
 Georgantopoulos I., Stewart G.C., Shanks T., Boyle B.J., Griffiths R.E., 1993, MNRAS, 262, 619
 Georgantopoulos I., Stewart G.C., Shanks T., Boyle B.J., Griffiths R.E., 1996, MNRAS, 280, 276
 Griffiths R.E., Georgantopoulos I., Boyle B.J., Stewart G.C., Shanks, T., Della Cecca, R., 1995, MNRAS, 275, 77
 Griffiths R.E., Della Ceca R., Georgantopoulos I., Boyle B.J., Stewart G.C., Shanks T., Fruscione A., 1996, MNRAS, 281, 71
 Hasinger G, Burg R, Giacconi R, Hartner G, Schmidt M, Trümper J, Zamorani G, 1993, AA, 275, 1
 Inoue H., Kii T., Ogasaka Y., Takahashi T., Ueda Y., 1996, in Roentgenstrahlung from the Universe, eds. Zimmermann U., Trumper, J.E., Yorke, H., MPE report 263, p. 323
 Ishisaki Y., 1996, Ph.D. thesis, University of Tokyo
 Kondo H., 1990, Ph.D. thesis, University of Tokyo
 Kraft R.P., Burrows D.N., Nousek J.A., 1991, ApJ, 374, 344

- Kubo H., Ikebe Y., Makishima K., 1994, ASCA newsletter No. 2
- Marshall F.E., Boldt E.A., Holt S.S., Miller R.B., Mushotzky R.F., Rose L.A., Rothschild R.E., Serlemitsos, P.J., 1980, ApJ, 235, 4
- Mather J.C. et al., 1990, ApJ, 354, L37
- Murdoch H.S., Crawford D.F., Jauncey D.L., 1973, ApJ, 183, 1
- Mushotzky, R.F., 1982, ApJ, 256, 92
- Nandra K., Pounds K.A., 1994, MNRAS, 268, 405
- Ohta K., Yamada T., Nakanishi K., Ogasaka Y., Kii T., Hayashida K., 1996, ApJ, 458, 570
- Piccinoti G. et al., 1982, ApJ, 253, 485
- Roche N., Shanks T., Georgantopoulos I., Stewart, G.C., Boyle B.J., Griffiths R.E., 1995, MNRAS, 273, L15
- Romero-Colmenero E., Branduardi-Raymont G., Carrera F.J., Jones, L.R., Mason K.O., McHardy I.M., Mittaz J.P.D., 1996, MNRAS, 282, 94
- Schmitt J.H.M.M., Maccacaro T., 1986, ApJ, 310, 334
- Serlemitsos P.J., Jalota L., Soong Y., Awaki H., Itoh M., Ogasaka Y., Honda H., Uchibori Y., 1995, PASJ, 47, 105
- Shanks T., Georgantopoulos I., Stewart G.C., Pounds K.A., Boyle B.J., Griffiths R.E., 1991, Nat, 353, 315
- Shanks T., Boyle B.J., 1994, MNRAS, 271, 753
- Soltan A., Hasinger, G., A&A, 1994, 288, 77
- Stark A., Gammie C.F., Wilson R.W., Bally J., Linke R.A., Heiles C., Hurwitz M., 1992, ApJS, 79, 77
- Stewart G.C., Georgantopoulos I., Boyle B.J., Shanks T., Griffiths, R.E., 1994, Makino, F. & Ohashi, T., Universal Academy Press, Tokyo, New Horizon in X-ray Astronomy: First results from ASCA, p. 331
- Takahashi T., Markevitch M., Fukazawa Y., Ikebe Y., Ishisaki, Y., Kikuchi K., Makishima K., Tawara Y., 1995, ASCA newsletter No. 3
- Tanaka Y., Inoue H., Holt S., 1994, PASJ, 46, L37
- Trümper J., 1990, Phys. Bl., 46, 137
- Vikhlinin A., Forman W., Jones C., Murray S., 1995, ApJ, 451, 553
- Vikhlinin A., Forman W., Jones C., Murray S., 1995b, ApJ, 451, 564
- Wood K.S., et al., 1984, ApJS, 56, 507